Biogeosciences Discuss., 6, 7017–7051, 2009
www.biogeosciences-discuss.net/6/7017/2009/

Biogeosciences Discussions

Biogeosciences Discussions is the access reviewed discussion forum of *Biogeosciences*

Regionalization of turbulent fluxes by combining aircraft measurements with footprint analysis

T. El-Madany[1], H. Geiß[2], A. Schmidt[1], and O. Klemm[1]

[1]University of Münster, Institute for Landscape Ecology, Robert-Koch-Straße 28, 48149 Münster, Germany
[2]Forschungszentrum Jülich GmbH, Institute of Chemistry and Dynamics of the Geosphere, ICG2 (Troposphere), 52425 Jülich, Germany

Received: 19 May 2009 – Accepted: 26 June 2009 – Published: 14 July 2009

Correspondence to: T. El-Madany (tarek.elmadany@uni-muenster.de)

Published by Copernicus Publications on behalf of the European Geosciences Union.

Abstract

This paper presents a method for the regionalization of turbulent fluxes by combining airborne flux measurements and footprint analysis. Eddy covariance measurements were performed with a small environmental research aircraft in May 2008 over the "Münsterland" region in northwest Germany. This region is dominated by agricultural patches that are typically a few hectares in size. An analytic footprint model was tested and applied to relate the fluxes, as measured on the aircraft during day time conditions, to different vegetation types on the ground. The geo referenced footprint areas were merged with high resolution land use data (30×30 m), resulting in a quantification of different land use types inside the respective footprints. The fluxes of the sampled area in the Münsterland of 1510 km^2 were scaled up to the area of the "Westfälische Bucht" (6054 km^2), since the land use composition are comparable to a large extent. The mean fluxes calculated of 99 flight segments and used for the regionalization were found $-0.69\,mg\,m^{-2}\,s^{-1}$ for carbon dioxide and $+0.17\,g\,m^{-2}\,s^{-1}$ for water vapor.

1 Introduction

Knowledge about nutrition and water cycles is of extraordinary importance for characterizing ecosystems and their role in the context of climate change. Especially sources and sinks of water vapor and carbon dioxide, the two single most important greenhouse gases, need to be quantified with high spatial and temporal resolution. A well developed understanding of these fluxes and the processes and parameters driving these fluxes will help to model the role of ecosystems and regions with respect to regional aspects of global change.

Cities are known to be sources of CO_2 as a result of human activity, as they concentrate traffic, power plants, industry and domestic heating. Their emission (and uptake) of green house gases including water vapor, is, however, difficult to model due to large variations in architecture, size, traffic, green belt and park areas, and the associated positive and negative feedback mechanisms. Although urban regions in Europe are densely covered with buildings and streets, significant portions resemble rural areas which act as a sink of carbon dioxide and, at the same time, as a source of water vapor. These rural areas are responsible for a significant contribution to the budget of CO_2 and H_2O even in the industrialized countries.

Eddy covariance is a method to estimate the turbulent exchange between surface and atmosphere. It is widely accepted and has been used since the early 1950's (Swinbank, 1951). Worldwide measurement networks have been established (Fluxnet; Wilson et al., 2002; Richardson et al., 2006, Ameriflux; Baldocchi et al., 2000; Falge et al., 2002, Carboeurop; Berbigier et al., 2001; Dolman et al., 2006, Asiaflux; Saigusa et al., 2002; Hirata et al., 2008 and Chinaflux; Fu et al., 2006; Yu et al., 2006) to quantify the energy and mass exchange between different vegetation types on the one hand and the atmosphere on the other. For various forest types (Yasuda et al., 2003; Li et al., 2005), agricultural crops (Kim et al., 2002; Moureaux et al., 2006), and natural vegetation (Nakai et al., 2008; Wohlfahrt et al., 2008) the carbon dioxide flux has been quantified by using tower-based applications of eddy covariance. Furthermore, flux measurements above cities (e.g. Grimmond et al., 2004; Schmidt et al., 2008) were employed to quantify the emission of carbon dioxide in urban areas.

Unfortunately, the areas captured by ground based flux towers only represent a limited section of an ecosystem or landscape. The respective measurement can be directly scaled up to larger areas only as long as the respective larger area is of identical vegetation type. To quantify the flux of CO_2 for a whole ecosystem or landscape, all aspects of the region have to be captured by the flux measurement. This is virtually impossible to be realized even with a large number of ground based experimental platforms.

One possibility to measure the CO_2 exchange of an entire ecosystem is to use a moving platform, as carried by a helicopter (Bange et al., 2006) or by an airplane (Graber et al., 1998; Gioli et al., 2006).

First attempts of airborne flux measurements have been made in the early 1980s

(Lenschow et al., 1980; Alvo et al., 1984; Desjardins et al., 1982). Since then measurement problems arising from the use of aircraft have been discussed by many authors. Desjardins et al. (1989) showed that means of consecutive flight segments are similar to a single long segment and that the flight direction with respect to the wind direction is important for flux measurements sampling at heights over 50 m above ground. Furthermore, Mann and Lenschow (1994) analyzed sets of short flights at different altitudes, and high-pass filtered time series and found that flux gradient errors and systematic flux errors are potentially large. A ground-speed correction for the time average was introduced by Crawford (1993), taking into account the aerodynamic characteristics of the airplane that correlate with the vertical wind speed. As a result, a spatial average is used instead of a time average. A model that estimates if an aircraft is suited to fly with rigid altitude control in a boundary layer with strong convection was presented by Busch et al. (1996). Strategies for obtaining adequate flux sampling by the use of repeated aircraft passes and grid patterns was developed by Mahrt (1998). Isaac et al. (2004) and Gioli et al. (2004) demonstrated that comparison of aircraft and ground based data show best agreement if flight height and sensor height are equal and if the footprint areas are of similar composition (e.g. vegetation and surface characteristics). In other words, great care must be taken if flux measurements from airborne platforms are interpreted in terms of surface fluxes.

So-called footprint models were developed to determine the surface area that contributes to the measured turbulent exchange. For example, at tower based sites, the vegetation directly underneath the tower does not contribute to the flux at the tower top at all, but the "source area" or "footprint" (Schmid, 2002) is located in the upwind direction of the tower. The function that describes the relationship between the spatial distribution of surface exchange flux and the measured signal at a certain height is the "source weight function" or "footprint function" (Schmid, 1997). Thus the source area or footprint can be interpreted as the integral of the source weight function or footprint function. Size and shape of the footprint vary with meteorological conditions such as wind speed and stability and are therefore highly time dependent.

Since the early 1990s, various footprint models were developed (Leclerc and Thurtell, 1990; Schuepp et al., 1990) to quantify the source areas contributing to experimentally determined fluxes (Schmid, 1997). There is a variety of models employing analytical forward (Horst, 2001; Kormann and Meixner, 2001) analytical backward (Kljun et al., 2002), and Lagrangian stochastical (Kurbanmuradov and Sabelfeld, 2000; Lee, 2003) approaches. They utilize different assumptions and approaches to model the respective footprint areas. Various meteorological data are used as input parameters to estimate the footprint function. The different models and their applications have been discussed and compared with each other by Schmid (2002) and Foken and Leclerc (2004) with the result that there is no optimum model. The model has to be chosen individually for each experimental site or instrumental approach.

2 Materials and methods

2.1 Meteorology

Meteorological measurement flights were conducted between May 21st and 24th 2008 above the "Münsterland" region in northwest Germany. The weather during the flight days was influenced by a moderately developed high pressure system with pressure between 1020 and 1015 hPa. The wind directions were from north to east. Cloud cover varied from 1/8 to 6/8 but it did not rain during the measurement period. Daily mean temperatures increased constantly from 12.6 to 16.7°C. The sun shine duration varied between 10 and 14 h per day. Wind speed was constant on the first three days, from 3 to 6 $m\,s^{-1}$. On the 24th the wind speed increased to up to 10 $m\,s^{-1}$.

2.2 Flight pattern

During the four measurement days eight flights with a total duration of 14 h and 34 min were performed. The flight pattern was designed to gather information about the CO_2

BGD
6, 7017–7051, 2009
Regionalization of turbulent fluxes by combining aircraft
T. El-Madany et al.

and H_2O fluxes of the city of Münster and its surrounding agricultural area. At the beginning and the end of each flight, vertical profiles were flown to analyze the height and vertical structure of the boundary layer, particularly with respect of the occurrence of temperature inversions and its turbulent mixing status. Due to federal restrictions and safety considerations, the flight height above the city was limited to a minimum of 300 m above ground. For the agricultural areas, a low-level flight permission allowed flight sections as deep as 50 m above ground.

2.3 Aircraft

A motor glider (ECO Dimona) endowed with fast response instruments for meteorological parameters and trace gases (Neininger et al., 2001; Schmitgen et al., 2004) was used to perform measurement flights around the city of Münster. The average operational cruising speed is between 40 m s^{-1} and 50 m s^{-1}, with the scientific payload used and full gasoline tanks the maximum endurance is about 5 h. The instruments are installed inside, or attached to the pods, which are mounted under the wings of the motor glider. Others are located inside the cockpit. The three dimensional wind speed is measured with a sensitive fast response five hole pressure probe as described in Crawford and Dobosy (1992). The water vapor concentrations are calculated with a combination of dew point mirror (Meteolabor) and an open path infrared gas analyzer (IRGA) (LI-COR 7500). The slow response (1 s) dew point mirror is for the exact concentration measurement and the IRGA to catch the fluctuations at 10 Hz. Carbon dioxide concentrations and fluctuations are derived in a similar way by using a combination of a closed path IRGA (LI-COR 6262) for concentrations and an open path IRGA for fluctuations. Furthermore, CO is measured with a fast response vacuum UV resonance fluorescence instrument as described by Gerbig et al. (1999). NO_2 is detected with a NOxTOy 6 channel Luminol detector (Dommen et al., 1999), O_3 is measured with a UV photometer and aerosols are measured with a laser particle counter.

2.4 Eddy covariance

The eddy covariance method was used to calculate the fluxes as measured with the airborne platform.

$$F = \overline{w'\varphi'} \quad (1)$$

F is the flux of a scalar, w the vertical wind speed, φ the scalar of interest, the prime denotes a deviation from the mean and the overbar indicates a mean over that time period. Straight and leveled flight segments were extracted for the flux calculation. To reduce the risk of measuring artificial fluxes which evoke from height gradients of the scalar of interest (Vickers and Mahrt, 1997; Mahrt, 1998), leveled segments with a standard deviation of less than 6 m of the flight height above sea level were used. Straight flight segments also assure that the airplane flies at a constant angle to the mean wind direction along each segment. This is a requirement for correct measurement of atmospheric turbulent fluxes, according to Taylor's frozen turbulence hypothesis (1938). Therefore, when flying straight segments, the airplane flies through differently sized eddies and captures them as a whole. Another aspect is that the airplane is horizontally leveled while flying straight, thus all instruments inside the left and right wing pods measure at the same height.

Kirby et al. (2008), Gioli et al. (2004), and LeMone et al. (2003) showed that an averaging length of four km is adequate to sample long enough wave components of the fluxes to represent the turbulent exchange. For this reason, the minimum length used for the flux calculation was set at 4 km.

Time series of temperature, H_2O and CO_2 were linearly detrended to eliminate artificial flux contributions that may occur when concentrations increase or decrease constantly due to events like advection of differently polluted air masses. The vertical wind speed was not detrended to maintain the turbulent structures of vertical air motion.

Crawford et al. (1993) showed that the use of a time average instead of a space average can lead to biases in the flux calculation of up to 20%. The space average is derived from a time series via:

$$[\varphi] = \frac{1}{\overline{S}T} \sum_i \varphi_i S_i \Delta t \qquad (2)$$

The square brackets indicate a space average of φ, where φ represents the vertical wind speed, temperature, water vapor, or carbon dioxide concentration. S is the speed of the aircraft, the overbar indicates an average over the time T (time of the flight segment), Δt is the time step between two measurement points and the subscript i refers to an instantaneous value.

Density fluctuations in the air result in apparent fluctuations of CO_2 and H_2O and thus have an effect on the calculated flux. This issue has to be addressed when using open path instruments. To eliminate this effect, Webb et al. (1980) introduced a correction term which was used in here.

2.5 Footprint model/footprint tool

To relate the fluxes as measured on the aircraft to their source area on the ground, the footprint tool of Neftel et al. (2008) was used. It is based on the footprint model of Kormann and Meixner (2001) and features a function for calculating footprint fractions related to predefined areas. A footprint fraction is a percentile contribution of a certain predefined area (in this study 1 km by 1 km squares, see below) inside the footprint, to the respective footprint. The footprint is represented by the area of an ellipse that is an approximation of the total area within the 1% isopleths of the maximum of the integrated footprint function (Neftel et al., 2008). This ellipse is used for the determination of the total footprint and will from now on be referred to as the footprint. The footprint is characterized by the displacement, i.e. the smallest distance of the 1% isopleths from the measuring point.

The footprint tool needs different types of input data: meteorological parameters (average wind speed for the flight segment, wind direction, standard deviation of the cross wind, Obukhov length L and friction velocity u_*), parameters describing the position

BGD

6, 7017–7051, 2009

Regionalization of turbulent fluxes by combining aircraft

T. El-Madany et al.

of the airplane (flight height above ground level and position of the airplane), and the coordinates of the predefined areas.

The Monin-Obukhov length L was calculated via:

$$L = -\frac{u_*^3}{k\frac{g}{\theta_v}\overline{w'\theta_v'}} \quad (3)$$

where u_* is the friction velocity, k the Von Karmann constant (0.4), g the acceleration due to gravity, θ_v the virtual potential temperature, and $\overline{w'\theta_v'}$ buoyancy flux at ground level.

The friction velocity u_* was calculated through the following formula:

$$\left[\left(\overline{u'w'}\right)^2 + \left(\overline{v'w'}\right)^2\right]^{1/4} \quad (4)$$

where u, v, and w are the three dimensional wind components, the primes refer to a deviation from the mean of the flight segment and the overbars denote a mean over the time of a flight segment.

One restriction for the footprint tool is that the value of z/L, which is an indicator for the atmospheric stratification, has to be between −3 and 3. This limitation is used in the footprint model because for a very unstable stratification (values of $z/L<-3$) the error of the velocity profile is unacceptably large (Kormann and Meixner, 2001). For values of $z/L>3$, the stability of the boundary layer is too high and turbulent exchange is inhibited thereby. In cases for which these conditions were not fulfilled, the respective footprint area was not calculated.

Usually, a footprint for fixed ground based flux measurements is calculated for the averaging period of the flux calculation (typically 30 min). For the aircraft, instead, for each time step of a flight segment, i.e. every 0.1 s, a footprint is generated and thus the footprints are overlapping each other (Fig. 1a). All input values for the footprint tool are averaged for the respective flight segment except for instantaneous wind direction and flight height.

By adding up all contributions of the predefined areas from the individual footprints, a total footprint is obtained for each flight segment. The percentile contribution of each predefined area to the total footprint is then computed. The result is a total footprint with spatial information about the flux contribution as shown in Fig. 1b.

In cases when the meteorological conditions are constant the contribution to the total footprint increases from the marginal areas to the center of the total footprint as shown in Fig. 1b. In cases of changing meteorological conditions, especially wind speed and wind direction, the maximum of the contribution appears smeared or even two local maxima may occur.

The spatial information, derived from the predefined areas (1 km×1 km), was spatially interpolated in Fig. 1b. To check the validity of the interpolation procedure above, the footprint contribution was calculated for a 250 m×250 m grid and compared to the 1 km×1 km grid results (Fig. 2). It can be seen that the major features of the footprint can be reproduced by the interpolation procedure. The approach for calculating the spatial information of the footprint was especially used for the evaluation of the footprint model for airborne flux measurements (Sect. 2.6).

2.6 Suitability of the footprint model/footprint tool for airborne flux measurements

From the perspective of a fast moving platform, the surface characteristics (forests, lakes, agricultural areas, and urban areas) captured by a footprint change from one footprint to another. In order to evaluate the suitability and correctness of the applied footprint model, specific “flux events” were compared with each other. A flux event in this sense is a short section of a $w'\varphi'$ time series, typically 2–4 s (about 100–200 m flight path) that has a high contribution to the averaged flux of the respective flight segment. During such time sections the landscape elements (lake, forest, urban area) that are accountable for the measured flux are represented by a few footprints (ca. 20–40). Only flux events within the same flight segment are compared to each other to assure that the meteorological conditions are comparable to each other as well as possible. Under these conditions, relative differences in the flux events can be attributed to different surface characteristics. Three major kinds of surfaces can be distinguished: vegetation surfaces that exhibit in an anti-correlation of $w'CO_2'$ and $w'H_2O'$, urban areas where traffic emissions lead to a positive CO_2 and NO_2 flux even at flight level, and water surfaces that have a positive impact on the H_2O flux. To illustrate this procedure an example is given in Sect. 3.1.

2.7 Regionalization of fluxes

Regionalization describes an up-scaling process of data measured at a point or within a small area (e.g. a couple of field plots) to a larger region. Up-scaling can only be realized if the sample area has at least the same characteristics (e.g. vegetation, soil and surface structure) as the area to which the information is to be scaled up to. This was assured by analyzing the land use inside the total footprint of a flight segment, and comparing it with the area that is supposed to be scaled up to. The land use types were derived through analysis of Landsat satellite data with a resolution of 30 m×30 m for the State of North Rhine Westphalia from the year 2005 (ZFL Universität Bonn, 2005). Twelve land use types were distinguished: three urban types depending on ratio of sealed areas (>80%, 80%–40%, <40%), deciduous forest, pine forest, mixed forest, arable land, grass land and meadow, water body sections, gravel pit mining, lignite open pit mining, and military training area (land use is blacked out).

2.8 Extraction and comparison of land use data

To combine the information from the land use data and the footprint data, geo information software (ArcGIS Version 9.3, ESRI Geoinformatik GmbH) was used. The routine involves six consecutive steps.

First, the ellipsis data from the footprint tool (length of the ellipsis axis, center coordinates, and rotation angle) are transformed into a geo referenced area by creating a shape file that contains all individual footprints that the total footprint of the respective

flight segment consists of. This is done with a tool (military analyst) that comes with the ArcGIS software.
Secondly, the land use data that fall into the total footprint of a flight segment are extracted from the entire land use dataset. The result is a land use map reduced to the size of the total footprint.

Thirdly, the land use type statistics inside the total footprint is calculated as a number of pixels representative for each land use type. The area of each land use type is calculated by multiplying the number of pixels with the area each pixel represents ($900\,m^2$).

Fourthly, when steps one to three are executed for all flight segments, the total land use that was captured by the flights is calculated. Therefore, land use data from all total footprints are added up and the percentile contribution for all land use types is calculated.

Fifthly, the percentile contribution of the land use types of the area that is supposed to be up-scaled, is calculated. This is done in the same manner as for the land use inside the total footprints.

Sixthly, the percentile contribution of the land use types is used to compare the composition of the sampled area and the area that is supposed to be scaled up. To the extent of which the compositions of the two areas are similar to each other up-scaling is considered possible.

2.9 Fluxes used for the regionalization

The flux data have to be of high quality to assure the accuracy for the regionalization. Therefore different criteria are more condensed than for simply applying the footprint model and additional criteria are introduced. Data are only used if a flight segment is longer than 4 km, the ratio of z/L is between −3 and 0.1 and the flight height is lower than 275 m above ground level. Analysis of segments longer than 4 km assure, that most of the flux contributing eddies are sampled (Sect. 3.3). A value of z/L between −3 and 0.1 assures that the stratification of the atmosphere is not stable and thus the exchange between surface and atmosphere (in flight height) is not inhibited. The flight height limitation assures that the airplane is well inside the mixing layer and thus the surface-atmosphere exchange can be measured correctly. The average of all fluxes that fulfill the restrictions mentioned above is used for the regionalization.

3 Results

3.1 Suitability of the footprint model for airborne flux measurements

The suitability of the footprint model for the interpretation of airborne flux measurements is of crucial importance. If the footprint model does not give a good representation of the source areas the regionalization of fluxes cannot be achieved. The source areas that influence turbulent exchange thus have to be characterized carefully in order to relate the measured, turbulent flux to land use types. In the following the flux events shown in Fig. 4 and Fig. 5 are discussed in combination with Fig. 3 to underline the differences in the flux events and the causes for these differences. Fig. 3 shows two typical flux events (grey shaded areas) in a 60 s extraction of the same flight segment. The first flux event is characterized by positive contributions to the CO_2, H_2O, and NO_2 fluxes. NO_2 is primarily from ground based, anthropogenic sources, traffic and other combustion processes. Thus it can be argued that the observed strong positive flux originated from the ground. The positive flux of H_2O is a result of evapotranspiration at vegetated areas. When looking at the concurrent positive NO_2, CO_2, and H_2O fluxes one would assume a footprint area that is dominated by heavy traffic ($w'NO_2'$ time series) but also includes some vegetated areas, as well as water bodies which both result in a positive H_2O flux too.

In this example anthropogenic emissions dominate the total CO_2 flux, while the vegetated areas are not large enough to take up all the emitted CO_2, but they influence the amplitude of the CO_2 flux. In Fig. 4 the footprint of the first flux event and a part of the $w'CO_2'$ time series including the flux event is shown. The wind direction for the time of this flux event was east. The colored squares represent the percentile contribution to the footprint of the flux event. The two areas that contribute together about 58% to the flux signal consist mainly of urban areas, a highly frequented autobahn, a bypass, and some major roads. Furthermore some green- and park areas are within this footprint area and many streets that are planted with trees can be found.

The second flux event occurs 15 s after the first one. The wind direction changed during this time from east to north north-east as shown in Fig. 3d. On the one hand the second flux event is characterized by high, positive NO_2 and H_2O fluxes, and on the other hand it is characterized by a strong, negative CO_2 flux. As for the first flux event the positive flux of the $w'H_2O'$ and $w'NO_2'$ time series indicate that the air masses are transported from the ground into the atmosphere. The strong anti-correlation between $w'CO_2'$ and $w'H_2O'$ shows that the air masses are dominated by the photosynthesis of the vegetation that takes up carbon dioxide and releases water vapor at the same time. Nevertheless the high values of the $w'NO_2'$ time series indicate, that the air mass was influenced by anthropogenic emissions too.

Figure 5 shows $w'H_2O'$-values of the above described segment, including the second flux event shown in Fig. 3. The areas that contribute 72% (51%, 15%, 6%) to the footprint of the flux event are strongly influenced by green areas including a forest, crops, grassland, shrubs and a lake. These green areas account for the strong anti-correlation of $w'CO_2'$ and $w'H_2O'$ and the high values of $w'H_2O'$ for the flux event. Urban areas that are also contained in the footprint contribute significant to the flux pattern. However, in contrast to the first event, the air was depleted of CO_2 by the vegetation, which results in a strong negative CO_2 flux. Applying this method, many flight segments where evaluated. A good agreement between the observed flux events and the composition of the footprint areas was found. Thus the footprint model is well suited for the determination of the footprint for airborne flux measurements under the premises used in this study.

3.2 Footprint analysis and land use data

The total footprint areas from the 99 flight segments add up to an area of 6947 km^2. The individual total footprint sizes vary between 13 km^2 and 268 km^2. The large differences in the total footprint sizes result from the differences in the flight segments length and micrometeorological parameters. The footprint area grows from unstable over neutral to stable stratification and with flight height above ground. The mean total footprint size is 70 km^2. The sample area is 1510 km^2 in size. Due to repetitive flight patterns the area of all total footprints is more than 4 times larger than the area of the "Münsterland" and the sample area, respectively. The area of the "Westfälische Bucht" is 6054 km^2. This is the regional landscape, in which the "Münsterland" is integrated and that is to be up-scaled to. The major land use type in the "Münsterland" region is arable land (over 50%). Meadows and grassland account for approximately 20%, forests (pine-, mixed-, and deciduous forests) for 15%, and the urban areas add up to 10% of the land use. The other land use types (water bodies, military training areas (land use is blacked out), lignite open pit mining, and gravel pit mining) add up to 1% of the land use. The percentile land use contribution for all total footprint areas, the sample area of the "Münsterland", and the "Westfälische Bucht" is very similar with differences of only a view percent (Fig. 6). Since the land use types, sampled by all total footprints, represent the composition of the "Münsterland" very well (Fig. 6) it can be assumed that the flux average is a representative value for the turbulent exchange of the "Münsterland".

3.3 Flux calculation from flight segments

Due to the restrictions mentioned in Sect. 2.4 and 2.9, 99 out of a total of 244 flight segments could be used for the flux calculation. The mean measurement height from the flight segments used for the flux calculation varied between 98 m and 275 m above ground level. The mean, minimum, maximum and standard deviation of the fluxes of CO_2, H_2O and sensible heat are represented in Table 1. The large standard deviation of the observed fluxes reflects the inhomogeneity of the surfaces with different compositions of vegetation, water surfaces, and urban areas. The strong anti-correlation of CO_2 and H_2O fluxes (Fig. 7, top) is a result of the vegetated areas that were sampled mostly. Since sensible heat, H_2O, and NO_2 have their sources on the ground their positive fluxes are indicators for the transport of air from the surface into the atmosphere. Thus a positive correlation can be observed between the fluxes of sensible heat and H_2O (Fig. 7, bottom) as well as for NO_2 (not shown). For all four measurement days the fluxes of CO_2, H_2O and sensible heat vary within the same range (Fig. 8, right side) even though the concentrations of CO_2, water vapor and the temperature change (Fig. 8, left side). This indicates that the influence of advective fluxes can be excluded on a time scale corresponding to the length of a flight segment. In a heterogeneous landscape with high spatial variability, any measured flux signal is influenced by the combined influence of various surface types (e.g. vegetation, water bodies, and urban areas). The averaging length of a flight segment, which is essential for the computation of reliable flux magnitudes, results in a blurred flux signal that cannot be related to certain source area types inside the footprint. Exemplarily a high contribution of a forest (45%) in a total footprint does not result in a more negative CO_2 flux than a small forest contribution (5%) (Fig. 9). As a result, when comparing the fluxes from the various flight segments with respect to the land use inside the footprints, there is no significant correlation between a certain land use type and the magnitude of the fluxes (Fig. 9). Nevertheless, for short time scales the contributing features can be identified. Examples for this are the flux events that can be related to small scaled land use types. Furthermore, there is no significant correlation of the measured fluxes with wind speed, wind direction, flight height or time of the day on a time scale of the flight segments (Fig. 10). This absence of significant correlation indicates that different combinations of the various parameters lead to the observed fluxes. The lack of correlation for the flight and meteorological parameters with the flux values shows that the turbulent exchange is not governed by any single parameter. The missing correlation between the flight segment distance and flux values indicates that the minimum length of 4 km is adequate for sampling the majority of the flux contributing eddies. This is also underlined by Fig. 11 that shows the spectral analysis of the vertical wind speed for three flight segments of different length. The mostly sampled eddies are in a range of 20–40 s for all three flight segments. Thus the longer flights capture eddies of similar size as compared to the shorter segments. Consequently the shorter segments do not miss eddies of larger sizes. Considering the speed of the airplane the apparent eddies are of about 1000–2000 m horizontal extent. The averaging length of the flight segments used for the flux calculation is therefore adequate.

4 Conclusions

In this study airborne measurements of turbulent exchange were regionalized by an analysis of footprint data and high resolution land use maps. We found that all requirements for a regionalization are fulfilled: the footprint model gives a good estimation of the source area; the land use type distribution inside the footprints and the up-scaled area are very similar to each other; the average period for the flux calculation was long enough to capture the relevant eddies. Thus, the measured values of the fluxes can be extrapolated to the area of the "Westfäliche Bucht" and give a quantitative estimate of the respective fluxes. The result is a mean carbon dioxide uptake by the different vegetation types of 4177 kg s^{-1} (± 2300 kg s^{-1}) for the area of the "Westfälische Bucht" (6054 km^2). The water vapor transferred into the atmosphere through evapotranspiration is 1029000 kg s^{-1} (±544000 kg s^{-1}). These average fluxes are representative for the growing period of late spring/early summer under day time conditions. Further investigations in this manner would certainly help to understand processes driving the turbulent fluxes on a regional scale. Moreover, quantification for the CO_2 uptake and the variance throughout the year would become feasible for a regional scale.

As the investigation of the footprint model showed, the footprint model by Kormann and Meixner (2001) is well suited for estimating the source area of the airborne flux measurements under the conditions used in this study. More investigations with specific tracers like SF_6 or CO from open fire could help to quantify the use of this footprint model under different conditions as used in this study.

The footprint fraction contribution to the footprint is a very useful feature of the footprint tool by Neftel et al. (2008). The tool should be developed further so it can be used for larger areas or whole regions.

Furthermore, a connection to a mesoscale chemical transport model would help to evaluate and verify the results achieved in this project.

Acknowledgements. Funding of the project by the EUFAR transnational access project REGAFLUXES is gratefully acknowledged. Further we thank B. Neininger and L. Müller for the maintenance of the instruments and operating the aircraft, and L. Harris for language-editing of the manuscript.

References

Alvo, P., Desjardins, R. L., Schuepp, P. H., and Macpherson, J. I.: Aircraft Measurements of CO2 Exchange over Various Ecosystems, Bound.-Lay. Meteorol., 29, 167–183, 1984.

Baldocchi, D., Finnigan, J., Wilson, K., Paw U, K. T., and Falge, E.: On measuring net ecosystem carbon exchange over tall vegetation on complex terrain, Bound.-Lay. Meteorol., 96, 257–291, 2000.

Bange, J., Zittel, P., Spiess, T., Uhlenbrock, J., and Beyrich, F.: A new method for the determination of area-averaged turbulent surface fluxes from low-level flights using inverse models, Bound.-Lay. Meteorol., 119, 527–561, doi:10.1007/s10546-005-9040-6, 2006.

Berbigier, P., Bonnefond, J. M., and Mellmann, P.: CO2 and water vapour fluxes for 2 years above Euroflux forest site, Agri. Forest Meteorol., 108, 183–197, 2001.

Busch, U., Hofmann, M., Jacobi, C., and Roth, R.: Errors in aircraft measurements of turbulent fluxes in a boundary layer with strong convection, Phys. Chem. Earth, 21, 393–397, 1996.

Crawford, T. L. and Dobosy, R. J.: A Sensitive Fast-Response Probe to Measure Turbulence and Heat-Flux from Any Airplane, Bound.-Lay. Meteorol., 59, 257–278, 1992.

Crawford, T. L., Mcmillen, R. T., Dobosy, R. J., and Macpherson, I.: Correcting Airborne Flux Measurements for Aircraft Speed Variation, Bound.-Lay. Meteorol., 66, 237–245, 1993.

Desjardins, R. L., Brach, E. J., Alvo, P., and Schuepp, P. H.: Aircraft Monitoring of Surface Carbon-Dioxide Exchange, Science, 216, 733–735, 1982.

Desjardins, R. L., Macpherson, J. I., Schuepp, P. H., and Karanja, F.: An Evaluation of Aircraft Flux Measurements of CO2, Water-Vapor and Sensible Heat, Bound.-Lay. Meteorol., 47, 55–69, 1989.

Dolman, A. J., Noilhan, J., Durand, P., Sarrat, C., Brut, A., Piguet, B., Butet, A., Jarosz, N., Brunet, Y., Loustau, D., Lamaud, E., Tolk, L., Ronda, R., Miglietta, F., Gioli, B., Magliulo, V., Esposito, M., Gerbig, C., Korner, S., Glademard, R., Ramonet, M., Ciais, P., Neininger, B., Hutjes, R. W. A., Elbers, J. A., Macatangay, R., Schrems, O., Perez-Landa, G., Sanz, M. J., Scholz, Y., Facon, G., Ceschia, E., and Beziat, P.: The CarboEurope regional experiment strategy, B. Am. Meteorol. Soc., 87, 1367–1379, doi:10.1175/Bams-87-10-1367, 2006.

Dommen, J., Prevot, A. S. H., Neininger, B., and Clark, N.: NOxTOy: A miniaturised new instrument for reactive nitrogen oxides in the atmosphere, Annual report PSI, 1999.

Falge, E., Tenhunen, J., Baldocchi, D., Aubinet, M., Bakwin, P., Berbigier, P., Bernhofer, C., Bonnefond, J. M., Burba, G., Clement, R., Davis, K. J., Elbers, J. A., Falk, M., Goldstein, A. H., Grelle, A., Granier, A., Grunwald, T., Gudmundsson, J., Hollinger, D., Janssens, I. A., Keronen, P., Kowalski, A. S., Katul, G., Law, B. E., Malhi, Y., Meyers, T., Monson, R. K., Moors, E., Munger, J. W., Oechel, W., U, K. T. P., Pilegaard, K., Rannik, U., Rebmann, C., Suyker, A., Thorgeirsson, H., Tirone, G., Turnipseed, A., Wilson, K., and Wofsy, S.: Phase and amplitude of ecosystem carbon release and uptake potentials as derived from FLUXNET measurements, Agric. Forest Meteorol., 113, 75–95, Pii S0168-1923(02)00103-X, 2002.

Foken, T. and Leclerc, M. Y.: Methods and limitations in validation of footprint models, Agric. Forest Meteorol., 127, 223–234, doi:10.1016/j.agrformet.2004.07.015, 2004.

Fu, Y. L., Yu, G. R., Sun, X. M., Li, Y. N., Wen, X. F., Zhang, L. M., Li, Z. Q., Zhao, L., and Hao, Y. B.: Depression of net ecosystem CO2 exchange in semi-arid Leymus chinensis steppe and alpine shrub, Agric. Forest Meteorol., 137, 234–244, doi:10.1016/j.agrformet.2006.02.009, 2006.

Gerbig, C., Schmitgen, S., Kley, D., Volz-Thomas, A., Dewey, K., and Haaks, D.: An improved fast-response vacuum-UV resonance fluorescence CO instrument, J. Geophys.Res. Atmos., 104, 1699–1704, 1999.

Gioli, B., Miglietta, F., De Martino, B., Hutjes, R. W. A., Dolman, H. A. J., Lindroth, A., Schumacher, M., Sanz, M. J., Manca, G., Peressotti, A., and Dumas, E. J.: Comparison between tower and aircraft-based eddy covariance fluxes in five European regions, Agric. Forest Meteorol., 127, 1–16, doi:10.1016/j.agrformet.2004.08.004, 2004.

Gioli, B., Miglietta, F., Vaccari, F. P., Zaldei, A., and De Martino, B.: The Sky Arrow ERA, an

innovative airborne platform to monitor mass, momentum and energy exchange of ecosystems, Ann. Geophys. Italy, 49, 109–116, 2006.
Graber, W. K., Neininger, B., and Furger, M.: CO2 and water vapour exchange between an alpine ecosystem and the atmosphere, Environ. Modell. Softw., 13, 353–360, 1998.
Grimmond, C. S. B., Salmond, J. A., Oke, T. R., Offerle, B., and Lemonsu, A.: Flux and turbulence measurements at a densely built-up site in Marseille: Heat, mass (water and carbon dioxide), and momentum, J. Geophys. Res. Atmos., 109, D24101, doi:10.1029/2004jd004936, 2004.
Hirata, R., Saigusa, N., Yamamoto, S., Ohtani, Y., Ide, R., Asanuma, J., Gamo, M., Hirano, T., Kondo, H., Kosugi, Y., Li, S. G., Nakai, Y., Takagi, K., Tani, M., and Wang, H. M.: Spatial distribution of carbon balance in forest ecosystems across East Asia, Agric. Forest Meteorol., 148, 761–775, doi:10.1016/j.agrformet.2007.11.016, 2008.
Horst, T. W.: Comment on 'Footprint analysis: A closed analytical solution based on height-dependent profiles of wind speed and eddy viscosity', Bound. Lay. Meteorol., 101, 435–447, 2001.
Isaac, P. R., Mcaneney, J., Leuning, R., and Hacker, J. M.: Comparison of aircraft and ground-based flux measurements during OASIS95, Bound.-Lay. Meteorol., 110, 39–67, 2004.
Kim, D. S., Harazono, Y., Baten, M. A., Nagai, H., and Tsuruta, H.: Surface flux measurements of CO2 and N2O from a dried rice paddy in Japan during a fallow winter season, J. Air Waste Manage., 52, 416–422, 2002.
Kirby, S., Dobosy, R., Williamson, D., and Dumas, E.: An aircraft-based data analysis method for discerning individual fluxes in a heterogeneous agricultural landscape, Agric. Forest Meteorol., 148, 481–489, doi:10.1016/j.agrformet.2007.10.011, 2008.
Kljun, N., Rotach, M. W., and Schmid, H. P.: A three-dimensional backward lagrangian footprint model for a wide range of boundary-layer stratifications, Bound.-Lay. Meteorol., 103, 205–226, 2002.
Kormann, R. and Meixner, F. X.: An analytical footprint model for non-neutral stratification, Bound.-Lay. Meteorol., 99, 207–224, 2001.
Kurbanmuradov, O. and Sabelfeld, K.: Lagrangian stochastic models for turbulent dispersion in the atmospheric boundary layer, Bound.-Lay. Meteorol., 97, 191–218, 2000.
Leclerc, M. Y. and Thurtell, G. W.: Footprint Prediction of Scalar Fluxes Using a Markovian Analysis, Bound.-Lay. Meteorol., 52, 247–258, 1990.
Lee, X.: Fetch and footprint of turbulent fluxes over vegetative stands with elevated sources,

Bound.-Lay. Meteorol., 107, 561–579, 2003.
LeMone, M. A., Grossman, R. L., Chen, F., Ikeda, K., and Yates, D.: Choosing the averaging interval for comparison of observed and modeled fluxes along aircraft transects over a heterogeneous surface, J. Hydrometeorology, 4, 179–195, 2003.
Lenschow, D. H., Delany, A. C., Stankov, B. B., and Stedman, D. H.: Airborne Measurements of the Vertical Flux of Ozone in the Boundary-Layer, Bound.-Lay. Meteorol., 19, 249–265, 1980.
Li, S. G., Asanuma, J., Kotani, A., Eugster, W., Davaa, G., Oyunbaatar, D., and Sugita, M.: Year-round measurements of net ecosystem CO2 flux over a montane larch forest in Mongolia, J. Geophys. Res. Atmos., 110, D09303 doi:10.1029/2004jd005453, 2005.
Mahrt, L.: Flux sampling errors for aircraft and towers, J. Atmos. Ocean. Tech., 15, 416–429, 1998.
Mann, J. and Lenschow, D. H.: Errors in Airborne Flux Measurements, J. Geophys. Res. Atmos., 99, 14519–14526, 1994.
Moureaux, C., Debacq, A., Bodson, B., Heinesch, B., and Aubinet, M.: Annual net ecosystem carbon exchange by a sugar beet crop, Agric. Forest Meteorol., 139, 25–39, doi:10.1016/j.agrformet.2006.05.009, 2006.
Nakai, Y., Matsuura, Y., Kajimoto, T., Abaimov, A. P., Yamamoto, S., and Zyryanova, O. A.: Eddy covariance CO2 flux above a Gmelin larch forest on continuous permafrost in Central Siberia during a growing season, Theor. Appl. Climatol., 93, 133–147, doi:10.1007/s00704-007-0337-x, 2008.
Neftel, A., Spirig, C., and Ammann, C.: Application and test of a simple tool for operational footprint evaluations, Environ. Pollut., 152, 644–652, doi:10.1016/j.envpol.2007.06.062, 2008.
Neininger, B., Fuchs, W., Baeumle, M., Volz-Thomas, A., Prevot, A. S. H., and Dommen, J.: A small aircraft for more than just ozone: MetAir's 'Dimona' after ten years of evolving development, 11th Symposium on Meteorological Observations and Instrumentation 81st American Meteorological Society Anual Meeting, Albuquerque, NM, USA, 14–19 January 2001, 2001.
Richardson, A. D., Hollinger, D. Y., Burba, G. G., Davis, K. J., Flanagan, L. B., Katul, G. G., Munger, J. W., Ricciuto, D. M., Stoy, P. C., Suyker, A. E., Verma, S. B., and Wofsy, S. C.: A multi-site analysis of random error in tower-based measurements of carbon and energy fluxes, Agric. Forest Meteorol., 136, 1–18, doi:10.1016/j.agrformet.2006.01.007, 2006.
Saigusa, N., Yamamoto, S., Murayama, S., Kondo, H., and Nishimura, N.: Gross primary production and net ecosystem exchange of a cool-temperate deciduous forest estimated by the

eddy covariance method, Agric. Forest Meteorol., 112, 203–215, Pii S0168-1923(02)00082-5, 2002.
Schmid, H. P.: Experimental design for flux measurements: matching scales of observations and fluxes, Agric. Forest Meteorol., 87, 179–200, 1997.
Schmid, H. P.: Footprint modeling for vegetation atmosphere exchange studies: a review and perspective, Agric. Forest Meteorol., 113, PII S0168-1923(0102)00107-00107, 2002.
Schmidt, A., Wrzesinsky, T., and Klemm, O.: Gap filling and quality assessment of CO2 and water vapour fluxes above an urban area with radial basis function neural networks, Bound.-Lay. Meteorol., 126, 389–413, doi:10.1007/s10546-007-9249-7, 2008.
Schmitgen, S., Geiss, H., Ciais, P., Neininger, B., Brunet, Y., Reichstein, M., Kley, D., and Volz-Thomas, A.: Carbon dioxide uptake of a forested region in southwest France derived from airborne CO2 and CO measurements in a quasi-Lagrangian experiment, J. Geophys. Res. Atmos., 109, D14302 doi:10.1029/2003jd004335, 2004.
Schuepp, P. H., Leclerc, M. Y., Macpherson, J. I., and Desjardins, R. L.: Footprint Prediction of Scalar Fluxes from Analytical Solutions of the Diffusion Equation, Bound.-Lay. Meteorol, 50, 353–373, 1990.
Swinbank, W. C.: The Measurement of Vertical Transfer of Heat and Water Vapor by Eddies in the Lower Atmosphere, J. Meteorol., 8, 135–145, 1951.
Vickers, D. and Mahrt, L.: Quality control and flux sampling problems for tower and aircraft data, J. Atmos. Ocean. Tech., 14, 512–526, 1997.
Webb, E. K., Pearman, G. I., and Leuning, R.: Correction of flux measurements for density effects due to heat and water-vapor transfer, Q. J. Roy. Meteor. Soc., 106, 85–100, 1980.
Wilson, K., Goldstein, A., Falge, E., Aubinet, M., Baldocchi, D., Berbigier, P., Bernhofer, C., Ceulemans, R., Dolman, H., Field, C., Grelle, A., Ibrom, A., Law, B. E., Kowalski, A., Meyers, T., Moncrieff, J., Monson, R., Oechel, W., Tenhunen, J., Valentini, R., and Verma, S.: Energy balance closure at FLUXNET sites, Agric. Forest Meteorol., 113, 223–243, Pii S0168-1923(02)00109-0, 2002.
Wohlfahrt, G., Anderson-Dunn, M., Bahn, M., Balzarolo, M., Berninger, F., Campbell, C., Carrara, A., Cescatti, A., Christensen, T., Dore, S., Eugster, W., Friborg, T., Furger, M., Gianelle, D., Gimeno, C., Hargreaves, K., Hari, P., Haslwanter, A., Johansson, T., Marcolla, B., Milford, C., Nagy, Z., Nemitz, E., Rogiers, N., Sanz, M. J., Siegwolf, R. T. W., Susiluoto, S., Sutton, M., Tuba, Z., Ugolini, F., Valentini, R., Zorer, R., and Cernusca, A.: Biotic, Abiotic, and Management Controls on the Net Ecosystem CO2 Exchange of European Mountain Grassland

Ecosystems, Ecosystems, 11, 1338–1351, doi:10.1007/s10021-008-9196-2, 2008.
Yasuda, Y., Ohtani, Y., Watanabe, T., Okano, M., Yokota, T., Liang, N. S., Tang, Y. H., Nik, A. R., Tani, M., and Okuda, T.: Measurement of CO2 flux above a tropical rain forest at Pasoh in Peninsular Malaysia, Agric. Forest Meteorol, 114, 235–244, Pii S0168-1923(02)00198-3, 2003.
Yu, G. R., Wen, X. F., Sun, X. M., Tanner, B. D., Lee, X. H., and Chen, J. Y.: Overview of ChinaFLUX and evaluation of its eddy covariance measurement, Agric. Forest Meteorol., 137, 125–137, doi:10.1016/j.agrformet.2006.02.011, 2006.
ZFL Universität Bonn: Landnutzungsklassifikation von NRW aus dem Jahr 2005, Ministerium für Umwelt und Naturschutz, Landwirtschaft und Verbraucherschutz, NRW, Bonn, 2005.

Table 1. Mean, minimum, maximum, and standard deviation (σ) of the carbon dioxide, the water vapor, and the sensible heat flux from all 99 flight segments between 21 May and 24 May.

Flux	Mean	Min.	Max.	σ
CO_2 (mg m^{-2} s^{-1})	−0.69	−1.6	−0.06	0.38
H_2O (g m^{-2} s^{-1})	0.17	0.01	0.44	0.09
Sensible heat (W m^{-2})	82	6.5	210	50

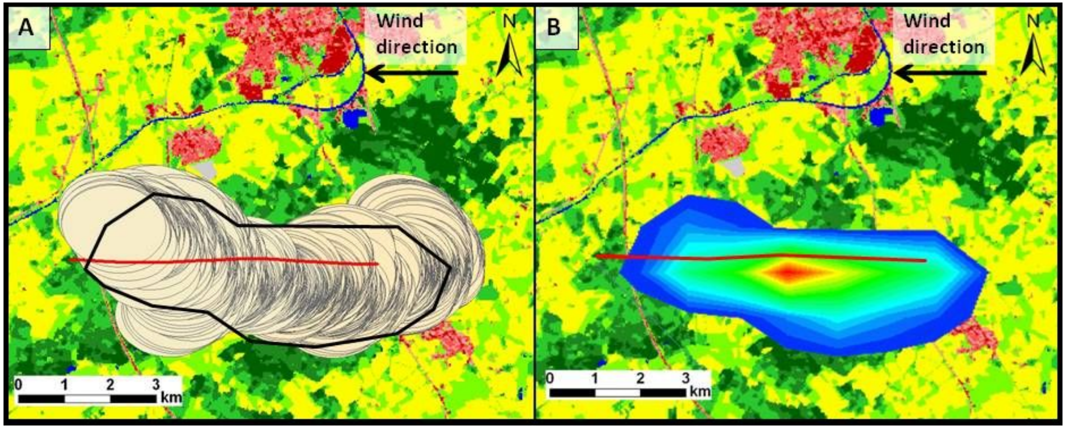

Fig. 1. (A) Land use map with all footprints (beige colored ellipses) of the flight segment. The black polygon represents the footprint of the right side, which was calculated from the ellipsis data of the left side. **(B)** A sketch of a footprint with interpolated, spatial information of the flux contribution. Colors represent the contribution of areas inside the footprint to the measured flux (from red (20%) to blue (1%) decreasing). The flight track of the aircraft is symbolized by a red line.

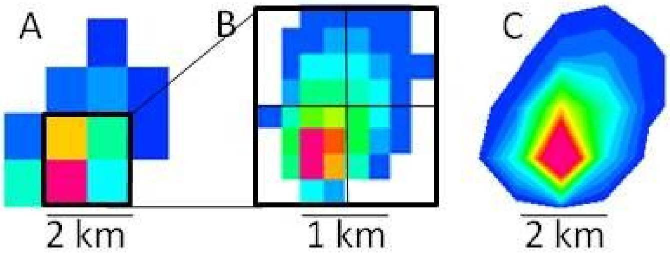

Fig. 2. Qualitative depiction of the spatial contribution of predefined areas to the footprint. Red color infers to high and blue to small contribution. **(A)** Footprint for a flux event with a square size for the predefined areas of 1 km×1 km. This footprint is described in more detail in Fig. 5. **(B)** The inner part of footprint A (inside the black square) is shown with a resolution of 250 m×250 m for the predefined areas. The white areas in A and B have less than 1% contribution to the footprint. **(C)** The same footprint as in A but spatially interpolated.

BGD
6, 7017–7051, 2009

Title Page
Abstract Introduction
Conclusions References
Tables Figures
◀ ▶
Back Close
Full Screen / Esc
Printer-friendly Version
Interactive Discussion

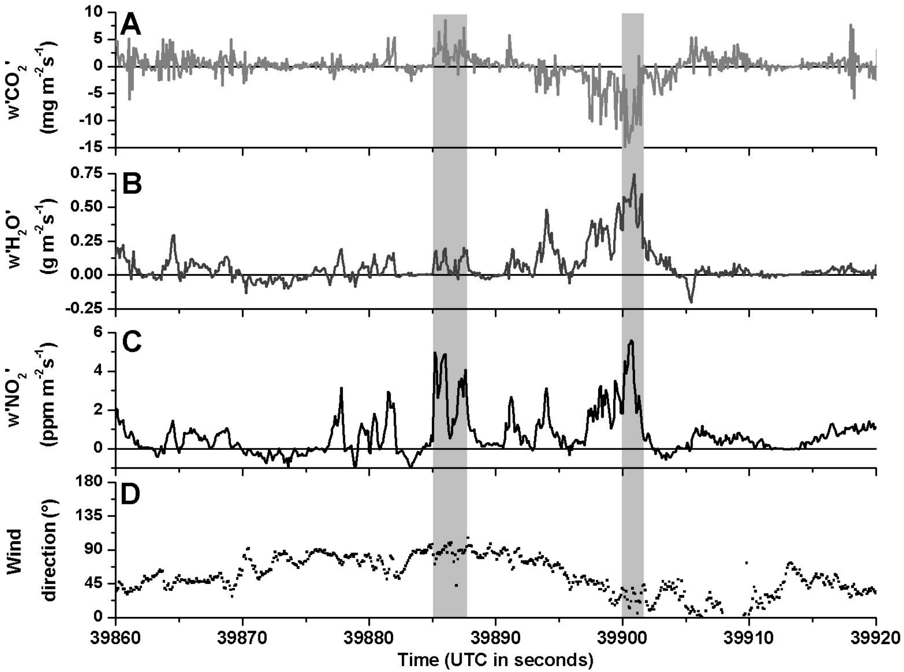

Fig. 3. A section of 60 s of a flight segment on 22.05.08 from east towards urban area. **(A)** $w'CO_2'$ time series in $mg\,m^{-2}\,s^{-1}$ **(B)** $w'H_2O'$ time series in $g\,m^{-2}\,s^{-1}$ **(C)** $w'NO_2'$ time series in $ppb\,m^{-2}\,s^{-1}$. **(D)** Wind direction in °. Grey shaded areas show flux events which are used in Fig. 4 (first highlight) and Fig. 5 (second highlight).

BGD

6, 7017–7051, 2009

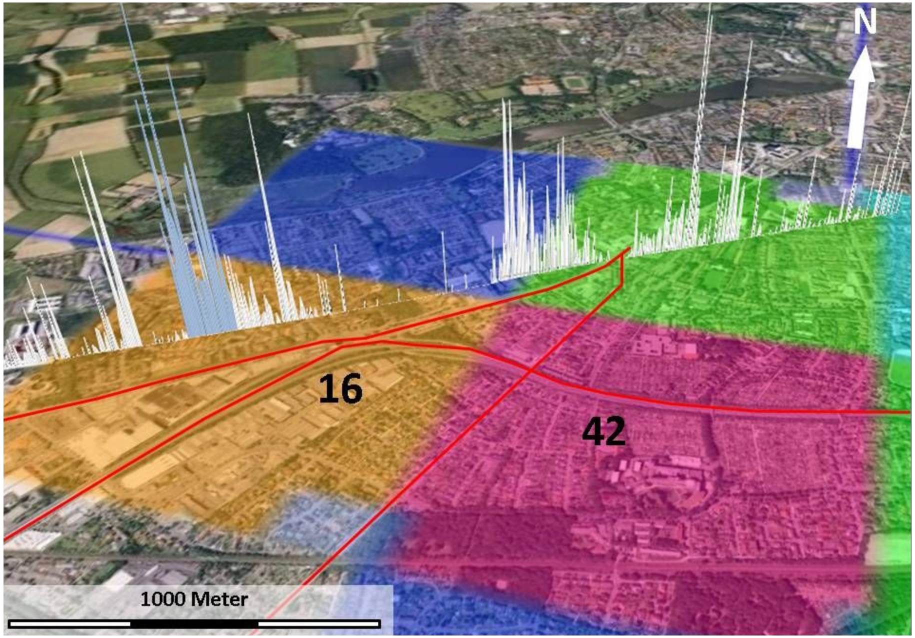

Fig. 4. Google Earth™ white areas show positive values of the $w'CO_2'$ plot of Fig. 3. The blue shaded area is the flux event that the footprint (colored squares) belongs to. The numbers inside the squares show the percentile contribution to the flux event. The red lines represent the autobahn, a bypass and major roads. The wind direction was east.

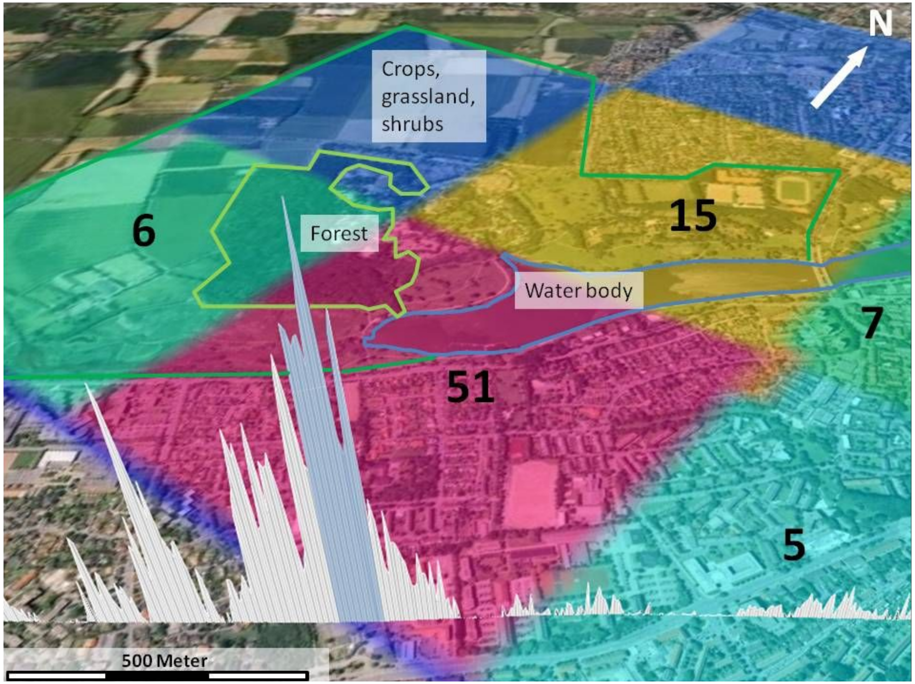

Fig. 5. Google Earth™ white areas show positive values of the $w'H_2O'$ plot of Fig. 3. The blue shaded area is the flux event that the footprint (colored squares) belongs to. The numbers inside the squares show the percentile contribution to the flux event. The wind direction was north north-east.

BGD

6, 7017–7051, 2009

Regionalization of turbulent fluxes by combining aircraft

T. El-Madany et al.

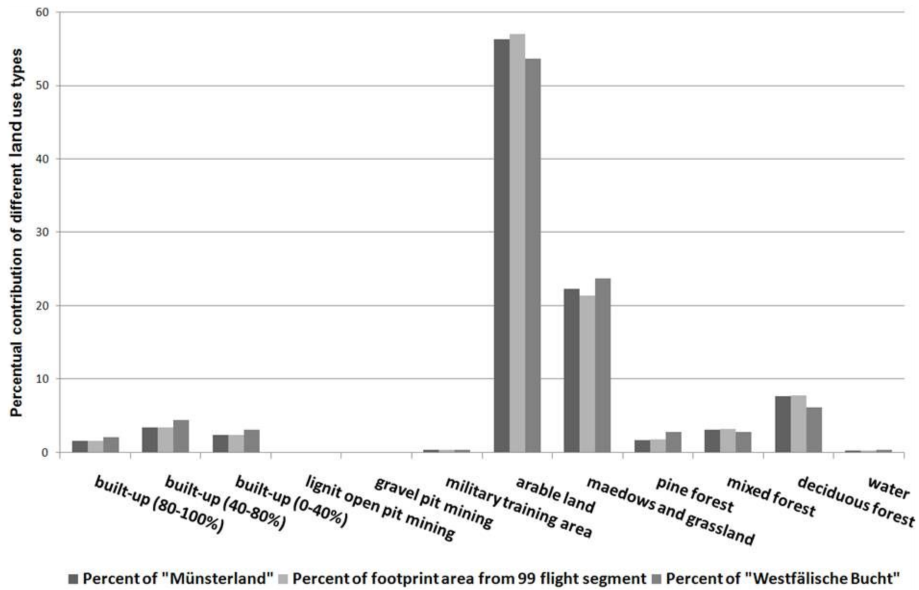

Fig. 6. Comparison of the land use contribution in all total footprints, the "Münsterland", and the "Westfälische Bucht".

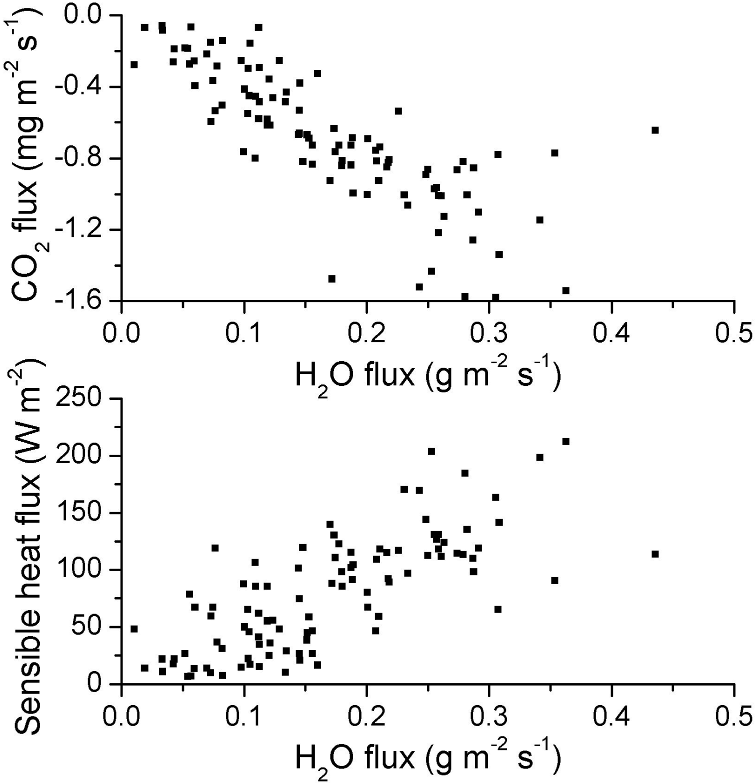

Fig. 7. Correlation between carbon dioxide fluxes and water vapor fluxes (top) and correlation of sensible heat fluxes and water vapor fluxes (bottom) from 99 flight segments.

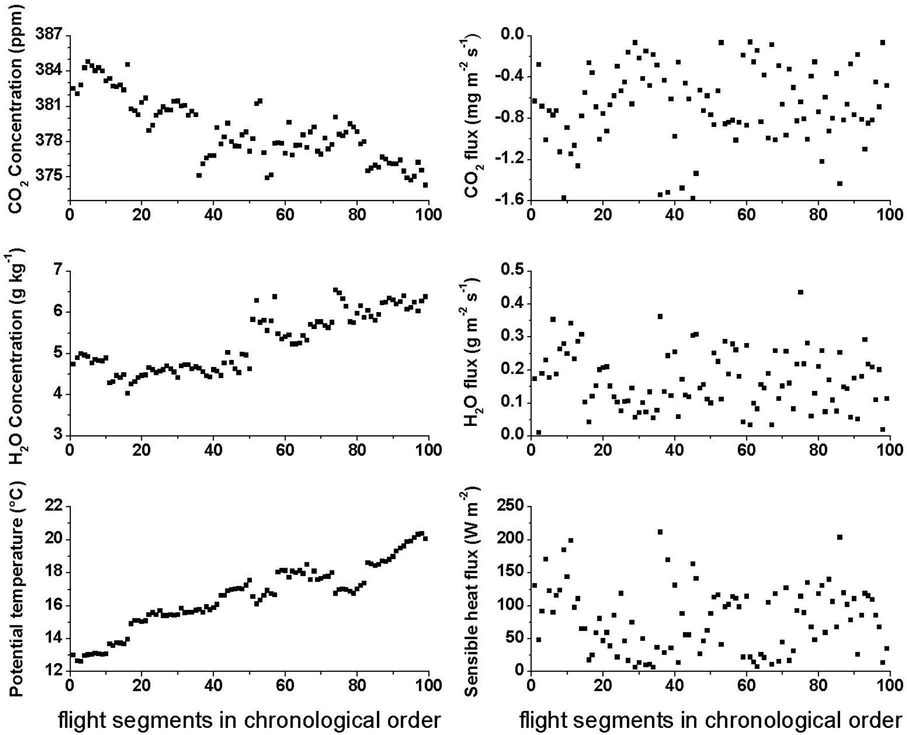

Fig. 8. Left side top to bottom: Means of carbon dioxide concentration, water vapor concentration, and potential temperature of the flight segments used for the flux calculation. Right side top to bottom: Carbon dioxide flux, water vapor flux, and sensible heat flux of the respective flight segments. The flight segment numbers are in chronological order beginning on 21 May and ending on 24 May.

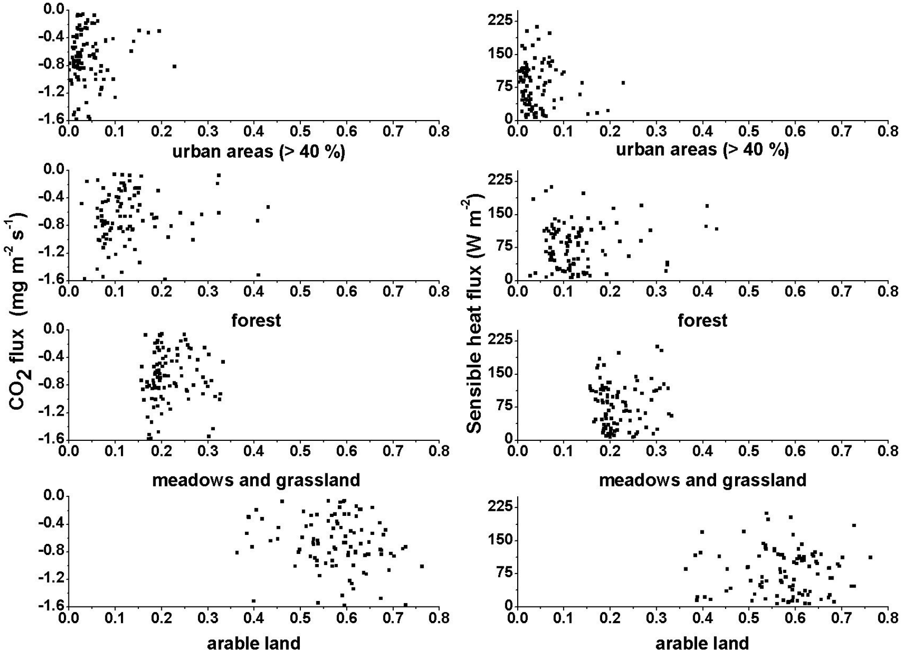

Fig. 9. Correlation of carbon dioxide flux (left) and sensible heat flux (right) to different land use type contributions.

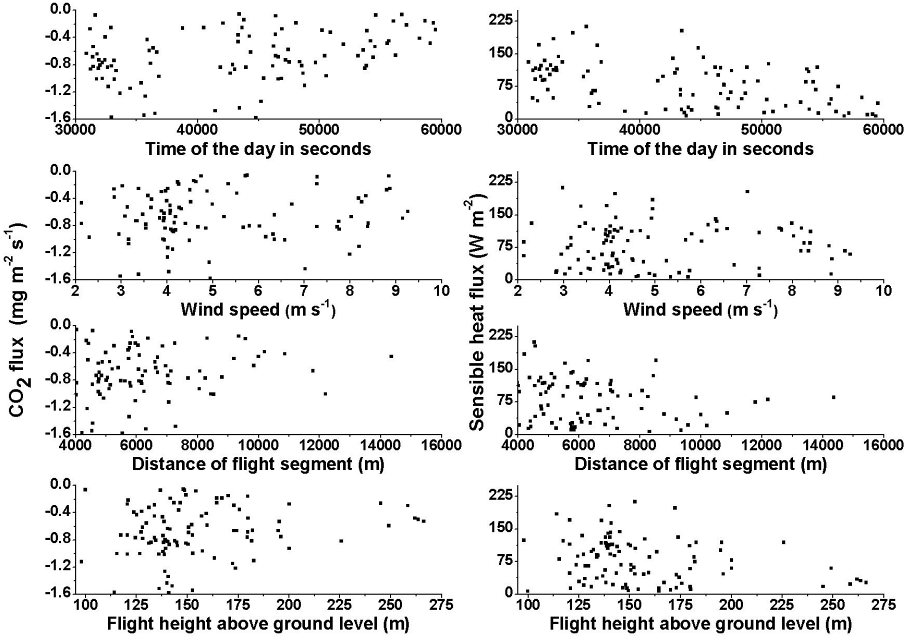

Fig. 10. Correlation of the carbon dioxide flux (left) and the sensible heat flux (right) to different meteorological and flight parameters.

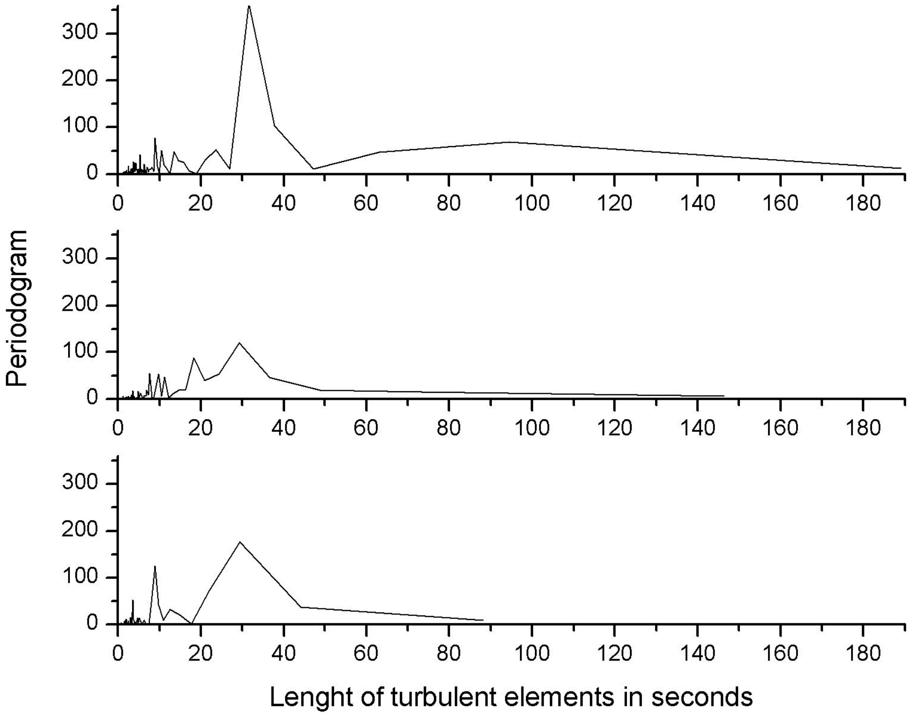

Fig. 11. Spectral analysis of three flight segments of different length. The duration of the flight segments is 189 seconds (top), 146 s (center), and 88 s (bottom).

BGD

6, 7017–7051, 2009

Regionalization of turbulent fluxes by combining aircraft

T. El-Madany et al.